Plasma Formation on the Front and Rear of Plastic Targets due to High-Intensity Laser-Generated Fast Electrons

M. Tatarakis,[1] J. R. Davies,[1] P. Lee,[1,*] P. A. Norreys,[2] N. G. Kassapakis,[1] F. N. Beg,[1] A. R. Bell,[1] M. G. Haines,[1] and A. E. Dangor[1]

[1]*Imperial College of Science, Technology and Medicine, London SW7 2BZ, United Kingdom*

[2]*Rutherford Appleton Laboratory, Chilton, Didcot, Oxon OX11 0QX, United Kingdom*

(Received 30 September 1997; revised manuscript received 5 March 1998)

Novel features of plasma generation by 1 ps, 1 μm, $\sim 10^{19}$ W cm^{-2} laser pulses on thick plastic targets are presented: (i) The electron distribution in the ablated plasma has a minimum along the target normal which persists long after the laser pulse (>1 ns); (ii) a narrow plasma jet is formed at the rear surface after a few picoseconds, in line with the laser focus. This is consistent with a beam of fast electrons traveling through the target, collimated by a magnetic field in the target. [S0031-9007(98)06636-8]

PACS numbers: 52.40.Nk

There has been much interest in high intensity laser-plasma interactions since the development of the chirped pulse amplification (CPA) technique [1,2] for generating short, high intensity laser pulses. This work has a number of applications [3]. One potential application is the "fast igniter" scheme [4] where it is proposed that fast electrons generated by a short laser pulse could be used to rapidly heat the core of a compressed DT fuel pellet to ignition. Here we present laser probing observations of the plasma at the front and rear surfaces of deuterated plastic (CD_2) targets in such interactions, which reveal interesting information on fast electrons.

The experiment used the CPA Vulcan glass laser at the Rutherford Appleton laboratory. The laser delivered a 1.054 μm wavelength, 30 J maximum energy, 1 ps duration, 3.5 times diffraction limited beam. A detailed description of the laser can be found in [5]. The p-polarized beam was focused at $f/4.5$ to a 12 μm diameter spot, giving a maximum intensity of 2.8×10^{19} W cm^{-2}, on 5 mm $\times$ 5 mm plastic slabs with thicknesses of 140–250 μm at 30° to the target normal. A small fraction, split from the uncompressed main beam, frequency doubled to the green (527 nm), and compressed to 1 ps, was used as a probe. The probe was passed transversely across the target, both the front and the back surfaces being in the field of view. Aspheric optics were used in the imaging system to give maximum spatial resolution of ~ 2 μm. The image plane was relayed outside the chamber and split into three. One beam was directed into a modified Nomarski interferometer [6], the second into a polarimeter, and the third into a shadowgraphic system. The acceptance angle of the optical system in all three channels was 0.12 radians ($f4$). Refraction of the probe in the strong density gradients limited observations to regions with electron density less than 10^{20} cm^{-3}. The probe beam was timed by decreasing the relative delay to a value such that no plasma was seen in the diagnostics. This was taken to be time zero.

Figure 1 shows some typical shadowgrams. The fringes are due to refraction in the steep density profile [7]. The bright spot at the target surface is present when the probe is switched off and is therefore due to second harmonic emission. The dark region immediately in front of the target, which is at a density greater than 10^{20} cm^{-3}, is seen to expand both normal to the target and along the target surface. Figure 2 is a plot of the expansion along the target normal as a function of time. Also shown in the inset are results from a MH2D (magneto-hydrodynamic two-dimensional) simulation [8], in which the laser is represented by heating at the critical surface. Ponderomotive effects and absorption into fast electrons are not included. The best fit to the data is for 15% laser absorption; 10% and 20% gave noticeably different results. This is consistent with the $\sim 10\%$ absorption into fast ions emitted from the front of targets reported in previous experiments [9]. The initial rapid expansion and agreement with the simulations shows that time zero does correspond with the arrival of the main pulse on the target. Results from previous experiments indicate that there is a short scale length (~ 1 μm) preplasma present [10]. Figure 3 shows interferograms at 5 and 81 ps, respectively, and the corresponding density contours obtained by Abel inversion. There is a density minimum along the target normal which forms a cone defined by the laser spot center on the target and a half angle of $\sim 16°$. This density minimum is sustained at late times. The shadowgram in Fig. 1(c) is recorded at 1.3 ns and clearly shows a density minimum at $r = 0$ at the tip of the plasma. The same effect has been observed by Attwood *et al.* [11] for a 3×10^{14} W cm^{-2}, 30 ps, 1.06 μm laser pulse but only during the laser pulse. A persistent density minimum, or channel, has been observed in experiments with preformed plasmas [12,13]. The density minimum on axis could be due to the ponderomotive force. Inclusion of radiation pressure in the MH2D simulations did not produce a density minimum; however, this simple

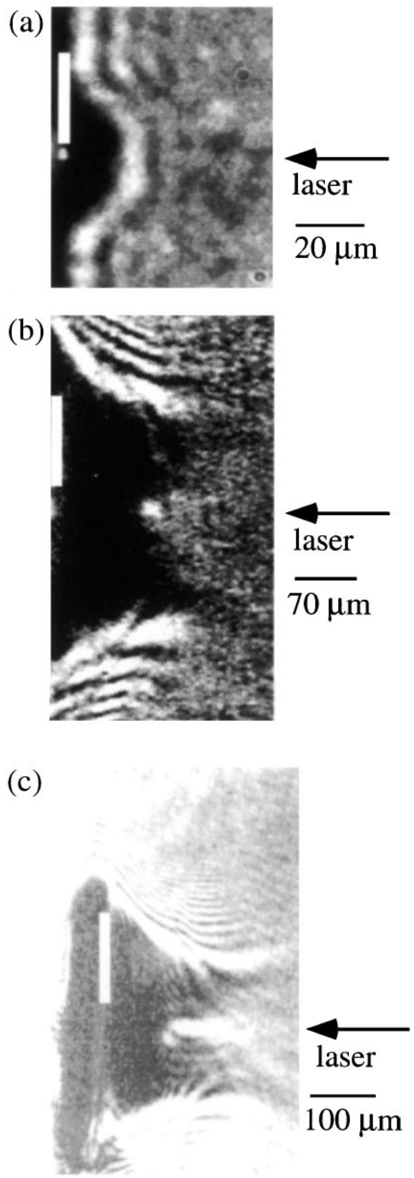

FIG. 1. Shadowgrams for (a) 22 ps, 11.5 J laser energy; (b) 450 ps, 13 J laser energy; and (c) 1300 ps, 13.4 J laser energy (CH target). The white line indicates the target surface. The bright spots, beneath the white lines, on the first two images are second harmonic emission (527 nm) which passes through the narrowband (527 ± 10) nm interference filter placed in front of the CCD detectors. The black region is the region inaccessible to the laser probe.

treatment cannot rule out this possibility. The cone angle agrees with that of the fast ion emission measured previously [8], indicating that this is the region which the ions are ejected from. Gitomer *et al.* [14] found a strong correlation between fast ions and fast electrons, showing that ions are ejected by electric fields generated by fast electrons. A cone angle of $\sim 16°$ is consistent with that found for fast electrons entering targets in numerous experimental and theoretical works, e.g., [15–20]. The polarimeter detected no rotation of the plane of polarization of the probe laser, indicating that it is $<1°$. This

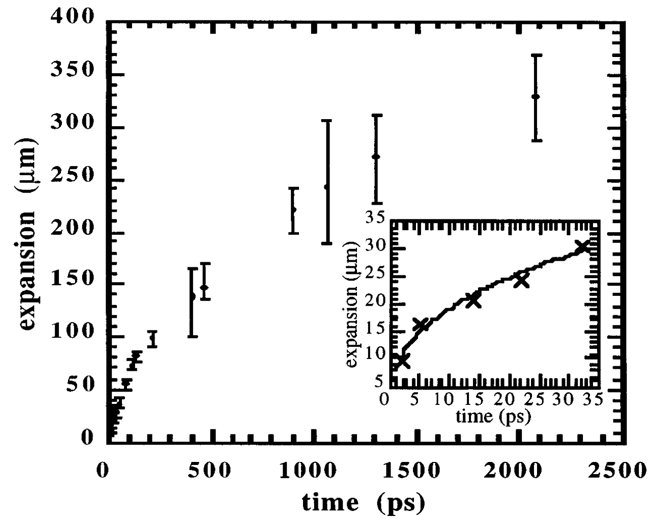

FIG. 2. Axial expansion (z) of the 10^{20} cm^{-3} contour along the target normal versus time. Each point is the average of 10 or more shots. The inset includes a line from a MH2D simulation for 15% absorption at the critical surface. The best fit to the experimental data is $z(\mu\text{m}) = 5.86 \times [t(\text{ps})]^{0.53}$.

corresponds to a magnetic field <200 T for an electron density of 5×10^{19} cm^{-3} and a distance of ~ 25 μm.

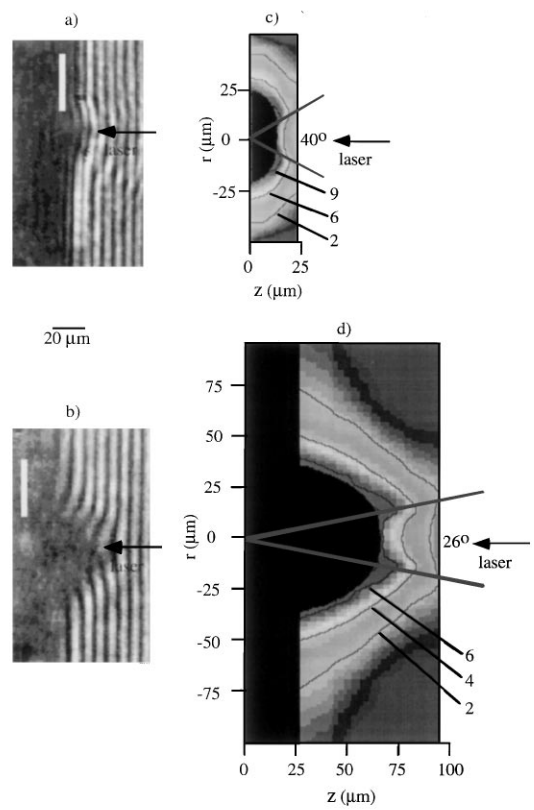

FIG. 3. Interferograms for (a) 5 ps, 14.5 J laser energy and (b) 81 ps, 14.2 J laser energy and the corresponding density contours [(c) and (d), respectively] in units of 10^{19} cm^{-3}. z is the distance along the normal from the target surface, which is marked with a white line, and r is the radial position from the laser spot center. Also shown is the full cone angle defined by the density wings.

Therefore the magnetic field does not exceed 200 T in regions accessible to the probe beam. The peak magnetic field in the MH2D simulations was ~100 T, and it was found to be important for the plasma hydrodynamics. A field <200 T is also consistent with the recent results of Mason and Tabak, where significantly higher fields were found in the overdense plasma [20]. Thus, the persistence of the density minimum could be due to a magnetic field.

Figure 4 gives two shadowgrams showing plasma at the rear surface. The earliest time that such a plasma was discernible was 22 ps with a 140 μm thick target [Fig. 4(a)]. It has a diameter of 6 ± 2 μm at the surface. It was present in all shadowgrams taken at later times for all targets [cf. Fig. 4(b)]. The plasma was always in line with the laser focal spot and expanded with time. We propose that this is formed by a beam of fast electrons, collimated by a magnetic field inside the target. Other mechanisms are either impossible or inconsistent with the observations. Transmission of the laser pulse through this thickness of solid is not possible. The prepulse at $\sim 10^{13}$ W cm^{-2} is above the target damage threshold and is absorbed. It precedes the main pulse by 300 ps, and in this time any plasma it formed was undetectable. It is unlikely that the leading edge of the prepulse is transmitted and then sharply focused at the rear of a target. To rule this out we carried out some shots with 50 μm thick aluminum slabs, which are opaque to 1 μm radiation, and a larger diameter, rear plasma was observed. Furthermore, if a 10^{13} W cm^{-2} laser pulse could generate this plasma it would have been observed in lower intensity experiments. Thus we can rule out formation by the prepulse. A formation time <22 ps immediately rules out transport around the target and shock breakout, which are inconsistent with the small diameter. The reproducible diameter and position and formation on aluminum rule out electrical breakdown due to fields generated at the front [21]. Transmission of fast ions (~MeV energies [8]) is ruled out by the target thickness.

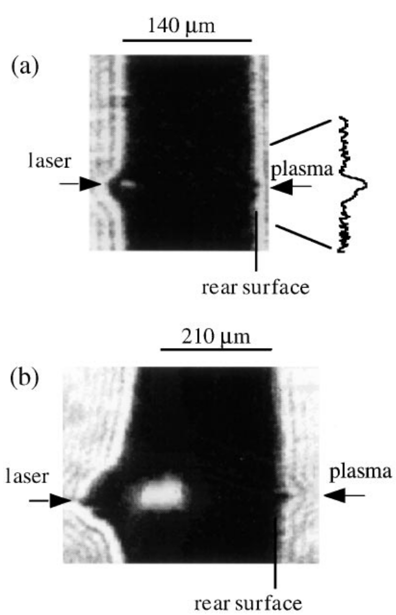

FIG. 4. Shadowgrams for (a) 22 ps, 11.5 J laser energy and (b) 207 ps, 20.2 J laser energy showing a plasma at the rear surface. The line in (a) gives a magnified trace of the rear surface of the region inaccessible to the probe.

This brings us to fast electrons. The measured fast electron temperature in [9] is 565 keV at 1.8×10^{19} W cm^{-2} (20 J laser energy). An electron with this kinetic energy has a speed of $0.88c$, so it can account for the rapid formation. The mean range of electrons in the target, as a result of angular scattering, is at most a factor of $\sqrt{6}$ (Z of carbon) lower than the stopping distance. An electron with a kinetic energy of 250 keV has a stopping distance $>\sqrt{6} \times 210$ μm [22]. This indicates that the bulk of the fast electrons will pass through the target with little energy loss. However, resistive inhibition could prevent penetration [23–25]. A mean penetration depth (z_0) from a 1D model including only the electric field is given in [25]. Using the Spitzer resistivity and the fast electron temperature from [9], this gives

$$z_0 \approx 0.0026\left(\frac{1}{f_{\mathrm{abs}}}\right)\left(\frac{T_b}{\mathrm{eV}}\right)^{3/2}\left(\frac{20}{Z \ln \Lambda}\right) \times \left(\frac{1.8 \times 10^{19}\ \mathrm{W\,cm^{-2}}}{I}\right)^{1/3} \mu\mathrm{m}\,, \qquad (1)$$

where T_b is the background temperature, f_{abs} is the absorption into fast electrons, and $Z \ln \Lambda$ is from the Spitzer formula [26]. This indicates that fast electron penetration will be prevented; however, this will lead to rapid heating of the background lowering the resistivity and allowing the fast electrons to penetrate further [27]. If $f_{\mathrm{abs}}(20\ \mathrm{J})$ heated every electron in a cylinder of CD_2 with a diameter of the laser spot and a length of 210 μm, T_b would be $f_{\mathrm{abs}}(10\ \mathrm{keV})$. This gives $z_0 = f_{\mathrm{abs}}^{1/2}(2600\ \mu\mathrm{m})$, and $z_0 > 210$ μm requires $f_{\mathrm{abs}} > 0.0065$. The absorption into the fast electrons is found to be ~40% [9]. If the electrons did spread out in the target, z_0 would be significantly increased from the 1D result due to the decrease in the current density, and the same results would apply. Thus, fast electrons are transmitted and can heat the target all the way through sufficiently to form a plasma at the rear. As they leave the rear surface they set up a space charge electric field which reflects them, forming an electron sheath at the surface with a scale length (d) given by the Debye length [28,29]. The electric field in this sheath is [29]

$$E \sim \frac{T_f}{d} \approx 1.3 \times 10^{-4}(n_f T_f)^{1/2}\ \mathrm{V\,m^{-1}}, \qquad (2)$$

where n_f and T_f are the number density and temperature (eV) of the fast electrons at the surface. As the surface is not a perfect conductor nor perfectly smooth, this field will affect it. Field ionization of hydrogen requires an electric field of 5×10^{11} V m^{-1}. Using $n_f T_f u_f = f_{\rm rear} f_{\rm abs} I/e$, where u_f is the fast electron speed and $f_{\rm rear}$ is the fraction of the generated fast electron flux leaving the rear surface, gives for $E > 5 \times 10^{11}$ V m^{-1}

$$f_{\rm rear} > 0.008\left(\frac{0.4}{f_{\rm abs}}\right)\left(\frac{1.8 \times 10^{19}\ {\rm W\,cm^{-2}}}{I}\right)\left(\frac{u_f}{0.88c}\right). \tag{3}$$

If the fast electrons propagated freely, then for this not to be satisfied they must be emitted into a full cone angle $>51°$ in the 140 μm target. To account for the diameter of the plasma observed they must have moved inwards; a 1° angle to the axis gives a 2.4 μm shift over 140 μm, comparable to the radius of the observed plasma. This can be explained by an azimuthal magnetic field in the target. This has been considered before [15,24,27]. It is generated by the finite radius of the axial electric field (from $\partial \mathbf{B}/\partial t = -\nabla \times \mathbf{E}$) generated by the fast electrons in the target, the cause of the resistive inhibition. Estimates of the magnetic field growth rate in this situation have been given in [24] and [27]; for our case we obtain

$$\frac{\partial B}{\partial t} \sim 1.3\left(\frac{f_{\rm abs}}{0.4}\right)\left(\frac{\rm keV}{T_b}\right)^{3/2}\left(\frac{Z \ln \Lambda}{20}\right) \times \left(\frac{I}{1.8 \times 10^{19}\ {\rm W\,cm^{-2}}}\right)^{2/3}\left(\frac{6\ \mu{\rm m}}{r_s}\right) kT\ {\rm ps}^{-1}, \tag{4}$$

where r_s is the spot radius. Thus a large magnetic field will be rapidly formed. The simulations given in [27] for aluminum, $I = 2 \times 10^{18}$ W cm^{-2} and $r_s = 10$ μm show significant magnetic field collimation. The higher intensity, smaller spot radius, and higher resistivity in our case would give a significantly higher magnetic field and the lower Z of the target a significantly lower spread due to angular scattering. Thus a high degree of collimation would be expected. Given that formation by fast electron transmission appears to be the only reasonable explanation, the experimental results show that the fast electrons are strongly collimated and give indirect evidence for the presence of a magnetic field in the target.

In conclusion, the plasma generated by a short, high-intensity laser pulse on plastic targets has been characterized by laser probing. The ablated plasma has a density minimum along the target normal which lasts long after the laser pulse. It corresponds with the region which fast ions are emitted from. Its persistence is most likely due to a magnetic field. This result is significant for the fast igniter as it indicates that a hole bored through the plasma will persist for long enough to guide the ignition pulse. The magnetic field in the underdense plasma is <200 T, in agreement with simulation. A plasma is formed at the rear surface after a few ps with a diameter less than that of the laser spot. This shows that fast electrons passing through the target are strongly collimated by an internal magnetic field. This is a very important result for the fast igniter as it would significantly increase the energy reaching the core. It also makes the laser alignment more critical as the electrons could miss the core altogether.

The authors gratefully acknowledge the assistance of Mr. F. N. Walsh during the experiment, Mr. C. Danson, and Dr. A. P. Fews for useful discussions and comments. This work was supported by the U.K. EPSRC (GR/K/9198) and by the European CEC contract (ERB-SCI*CT000728).

*Present address: Electrical and Electronic Engineering, Nanyang Technological University, Singapore 639798.

[1] D. Strickland and G. Mourou, Opt. Commun. **56**, 219 (1985).
[2] P. Maine *et al.*, IEEE J. Quantum Electron. **24**, 398 (1988).
[3] P. Gibbon and E. Forster, Plasma Phys. Controlled Fusion **38**, 769 (1996).
[4] M. Tabak *et al.*, Phys. Plasmas **1**, 1626 (1994).
[5] C. N. Danson *et al.*, Opt. Commun. **103**, 392 (1993).
[6] R. Benattar, C. Popovics, and R. Sigel, Rev. Sci. Instrum. **50**, 1583 (1979).
[7] R. Benattar and C. Popovics, J. Appl. Phys. **54**, 603 (1983).
[8] A. R. Bell *et al.*, Phys. Rev. E **48**, 2087 (1993).
[9] F. N. Beg *et al.*, Phys. Plasmas **4**, 447 (1996).
[10] P. A. Norreys *et al.*, Phys. Rev. Lett. **76**, 1832 (1996).
[11] D. T. Attwood *et al.*, Phys. Rev. Lett. **40**, 184 (1978).
[12] M. Borghesi *et al.*, Phys. Rev. Lett. **78**, 879 (1997).
[13] J. Fuchs *et al.*, Phys. Rev. Lett. **80**, 1658 (1998).
[14] S. J. Gitomer *et al.*, Phys. Fluids **29**, 2679 (1986).
[15] B. Luther-Davies, A. Perry, and K. A. Nugent, Phys. Rev. A **35**, 4306 (1987).
[16] S. C. Wilks *et al.*, Phys. Rev. Lett. **69**, 1383 (1992).
[17] S. C. Wilks, Phys. Fluids B **5**, 2603 (1993).
[18] A. Rousse *et al.*, Phys. Rev. E **50**, 2200 (1994).
[19] A. Pukhov and J. Meyer-ter-Vehn, Phys. Rev. Lett. **79**, 2686 (1997).
[20] R. J. Mason and M. Tabak, Phys. Rev. Lett. **80**, 524 (1998).
[21] F. Amiranoff *et al.*, Phys. Rev. A **32**, 3535 (1985).
[22] International Committee on Radiation Units Report No. 37, 1984.
[23] R. B. Miller, *An Introduction to the Physics of Intense Charged Particle Beams* (Plenum Press, New York, 1982), Chap. 4.
[24] M. E. Glinsky, Phys. Plasmas **2**, 2796 (1995).
[25] A. R. Bell *et al.*, Plasma Phys. Controlled Fusion **39**, 653 (1997).
[26] L. Spitzer, *Physics of Fully Ionised Gases*, edited by R. E. Markshak (Interscience Publications, New York, London, 1962).
[27] J. R. Davies *et al.*, Phys. Rev. E **56**, 7193 (1997).
[28] H. Hora, *Physics of Laser Driven Plasmas* (Wiley, New York, Chichester, 1981).
[29] J. R. Davies, Ph.D. thesis, Imperial College, University of London, U.K., 1997; M. Tatarakis, Ph.D. thesis, Imperial College, University of London, U.K., 1997.